Proceedings of the 12th International Symposium on Physics of Materials, Prague, September 4–8, 2011

Topological Model of Austenite–Martensite Interfaces in Cu–Al–Ni Alloy

A. Ostapovets, N. Zarubova and V. Paidar*

Institute of Physics ASCR v.v.i, Na Slovance 2, Prague 8, Czech Republic

Discussion of the austenite–single-variant martensite interfaces in Cu–Al–Ni alloy is performed in the frame of a topological model of martensite interfaces. This model takes into account admissible defects lying in the interface. The results are compared with the experimental data obtained on the foils of Cu–Al–Ni alloys deformed *in situ* in a transmission electron microscope.

PACS: 63.70.+h

1. Introduction

Cu–Al–Ni alloy is one of the most widely studied shape-memory alloys because of a very large reversible strain and relative easiness of single crystal preparation. The β_1 austenite phase has DO_3 structure with the lattice parameter of 0.5836 nm. Three types of martensite are observed in this alloy: γ_1' with $2H$, β_1' with $18R$, and α_1' with $6R$ structures. The orthorhombic γ_1' martensite has the lattice parameters $a = 0.4382$ nm, $b = 0.5356$ nm, and $c = 0.4222$ nm [1].

The experiments indicate that flat interfaces between the austenite and a single variant of $2H$ martensite can exist on a microscopic scale [2]. Unfortunately, no invariant plane can be found for martensitic transformations in this material [3]. Consequently, the classical phenomenological theory of martensite cannot predict interface plane between the austenite and a single variant of $2H$ martensite. It is possible to find only an average macroscopic habit plane between the austenite and two twin-related martensite.

The flat interfaces between the austenite and single variant of the martensite were discussed in our previous paper [4] where a simple shear strain of martensite was included in the phenomenological model in order to find the invariant plane. A comparatively large set of possible habit planes was obtained in that way and it was shown that this set is not in contradiction with the experimental results. However, the simple shear deformation of martensite was included in the model in a purely mathematical way without physical justification.

The aim of the present paper is to discuss the austenite–single-variant-martensite interfaces in Cu–Al–Ni alloy in the frame of topological model of martensite interfaces [5–7]. This model takes into account admissible defects lying in the interface. Hence, it allows prediction of the austenite–martensite habit planes only by analysis of such defects without considerations of the invariant plane.

* corresponding author; e-mail: paidar@fzu.cz

2. Model

2.1. Topological model

Topological model of martensite interfaces was developed by Pond and co-workers and its detailed description can be found in [5–7]. The model considers the structure of austenite–martensite interface in the following way. It is supposed that such interface contains coherent terraces with superimposed arrays of defects. These arrays of defects accommodate coherency strains i.e. they allow the crystal to be strained in order to satisfy the coherency of terraces. At least two arrays of defects are considered. One of them consists of transformation dislocations or disconnections, and another one contains defects of lattice invariant deformation (LID). LID defects are slip or twinning dislocations in the martensite phase.

In order to find the structure of austenite–martensite interface, following steps have to be performed:

— Selection of possible coherent terraces. Since austenite and martensite phases are typically associated with certain orientation relationship, it is possible to select terrace planes as corresponding planes in both phases. Coherency strains have to be small in these planes.

— Selection of possible interfacial defects in the terrace planes. Burgers vector b and step height h of such defects are defined by the symmetries of austenite and martensite phases.

— The arrays of interfacial defects necessary to accommodate the coherency strain are determined in terms of directions of defect lines ξ^D and ξ^L and their spacings d^D and d^L.

2.2. Crystallography

Three types of twinning occur in Cu–Al–Ni $2H$ martensite [3, 8]:

type-I: $K_1 = \{121\}_M$, $\eta_1 = [\bar{1}\ 0.7947\ \overline{0.5893}]_M$,
$K_2 = (\bar{1}\ 1.5036\ \overline{0.5036})_M$, $\eta_2 = [111]_M$;

type-II: $K_1 = (\bar{1}\ 1.5036\ \overline{0.5036})_M$, $\eta_1 = [111]_M$,
$K_2 = (121)_M$, $\eta_2 = [\bar{1}\ 0.7947\ \overline{0.5893}]_M$;

compound: $K_1 = (101)_M, \quad \eta_1 = [\bar{1}01]_M,$
$K_2 = (\bar{1}01)_M, \quad \eta_2 = [101]_M.$

Here K_1 is the twinning plane and η_1 is the direction of the twinning shear. These types of twinning can be considered as LID deformation.

Six variants of martensite are possible with different orientations relative to the austenite phase. Let us limit our consideration to the boundary between austenite and $V3$ variant of martensite [2]. The interfaces between austenite and other variants can be obtained from symmetry considerations. The $V3$ variant has the following orientation relationship to austenite:

$$[100]_M||[10\bar{1}]_A; \; [010]_M||[010]_A; \; [001]_M||[101]_A. \quad (1)$$

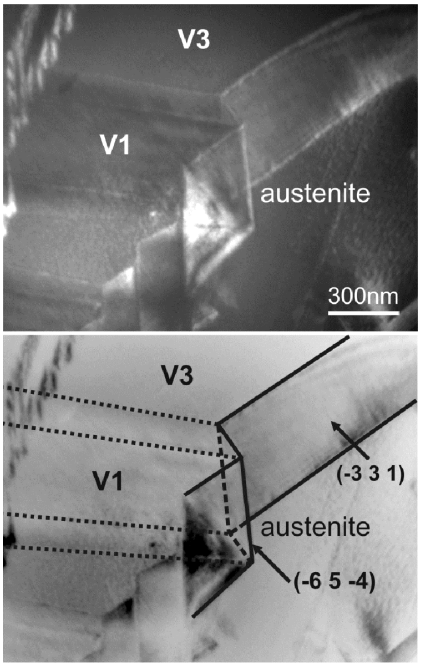

Fig. 1. (a) TEM micrograph of the boundary between β_1 austenite and the twinned γ_1' martensite. Dark field, reflection $202\beta_1$. (b) A scheme of the β_1/γ_1' boundary. It is formed by the segments of $(\bar{3}31)_A$ and $(\bar{6}5\bar{4})_A$ planes in this case.

The type-I twinning is considered as LID deformation. The choice of this type of interface is motivated by the fact of suitable experimental results for comparison [2]. An example of experimental austenite–martensite interface is shown in Fig. 1, where the interface plane for $V3$ variant is $(\bar{3}31)_A$. However other planes of interfaces are also observed. The experimentally observed austenite–$V3$ martensite planes are $(\bar{7}\ 13\ 9)_A$, $(\bar{7}54)_A$, $(\bar{3}31)_A$, $(1\bar{1}\ 18\ 11)_A$, $(\bar{2}54)_A$ [2, 3].

3. Results and discussion

3.1. Coherency strains

The first intuitive choice of candidate terrace planes can be the $\{110\}_A$ and $\{001\}_M$ planes in austenite and martensite, respectively. These planes are nearly parallel. Besides, $\{101\}_A$ is the most dense plane in the bcc based DO_3 structure. However this is not the best choice because it obviously does not agree with the experimental results [2, 3]. It is expected that the inclination of the habit plane from the terrace plane will be $\approx 10°-20°$ [5] but the inclination of $\{101\}_A$ plane from the experimental interfaces is much larger. Therefore, selection of candidate terrace planes $\{110\}_A$ and $\{1\bar{2}1\}_M$ is more appropriate. The orientation relationship $(110)_A[1\bar{1}\bar{1}]_A||(121)_M[2\bar{1}0]_M$ is reported in the literature for Cu–Al–Ni alloy [1]. Four symmetrically equivalent relationships are possible in the case of $V3$ variant with orientation (1):

$(110)_A[\bar{1}11]_A||(121)_M[\bar{2}10]_M;$

$(011)_A[11\bar{1}]_A||(\bar{1}21)_M[210]_M;$

$(0\bar{1}1)_A[\bar{1}11]_A||(\bar{1}\bar{2}1)_M[\bar{2}10]_M;$

$(1\bar{1}0)_A[11\bar{1}]_A||(1\bar{2}1)_M[210]_M.$

The atom configurations in coherently strained $\{110\}_A$ and $\{121\}_M$ planes are shown in Fig. 2. $\{121\}_M$ plane in martensite is corrugated and is split into two sub-planes [9]. Only one of this sub-plane is shown in Fig. 2 for simplicity.

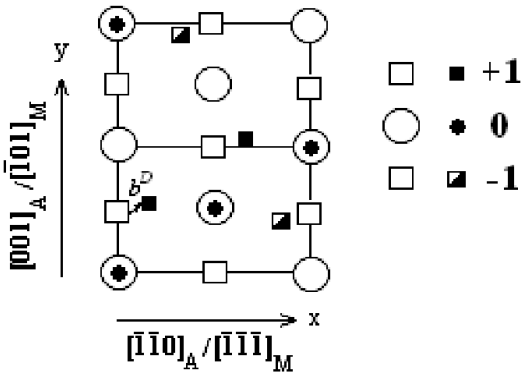

Fig. 2. Coherently strained $\{110\}_A$ (white) and $\{121\}_M$ (black) planes. Only one of corrugated $\{121\}_M$ sub-planes is shown. Projection in the $[110]_A$ direction of austenite. A possible Burgers vector of admissible defect is shown by the arrow.

According to [7] it is possible to write 2×2 matrices representing the deformation of austenite (P_c) and martensite (M_c) to the coherent state. The matrices in the xy coordinate system shown in Fig. 2 are

$$P_c = \begin{pmatrix} 0.991 & -0.0145 \\ 0 & 1.021 \end{pmatrix}, \quad (2)$$

$$M_c = \begin{pmatrix} 1.0088 & 0.0143 \\ 0 & 0.9793 \end{pmatrix}, \quad (3)$$

$$E_c = \left(P_c^{-1} - M_c^{-1}\right) = \begin{pmatrix} 0.0178 & 0.0288 \\ 0 & -0.0417 \end{pmatrix}. \tag{4}$$

3.2. Interfacial defects

A possible disconnection Burgers vector $\boldsymbol{b}^D$ is indicated by the arrow in Fig. 2. Projection of the disconnection Burgers vector on the xy plane is $\boldsymbol{b}^D = [0.2609, 0.0483]$ and the step height is $h(A) = 0.206$ nm and $h(M) = 0.201$ nm in austenite and martensite, respectively.

The second array of defects has to be an array of LID. There are twinning dislocations in the considered case. The Burgers vector of possible type-I twinning dislocation has to lie close to η_1 and is equal to the difference of two translation vectors — one in the matrix and another one in the twin. It seems that the best choice is $\boldsymbol{b}^L \approx 1/32\langle\bar{5}4\bar{3}\rangle_M$. The length of this vector is 1.05 Å and it is inclined from irrational η_1 by 0.24°. Corresponding translation vectors are $t_1 = [010]_M$ and $t_2 = [\bar{1}0\bar{1}]_M$ in the matrix and twin, respectively.

3.3. Interface structure

The directions of defect lines ξ^D and ξ^L and their spacings d^D and d^L can be found by substitution to the equations from [7]:

$$\boldsymbol{\xi}^D = \frac{\pm(E_c)^{-1}\boldsymbol{b}^L}{\left|(E_c)^{-1}b^L\right|}, \tag{5}$$

$$\boldsymbol{\xi}^L = \frac{\pm(E_c)^{-1}\boldsymbol{b}^D}{\left|(E_c)^{-1}b^D\right|}, \tag{6}$$

$$d^D = \frac{\left|\boldsymbol{b}^D\right|}{\left|E_c\boldsymbol{\xi}^L\right|}\sin\left|\theta^D - \theta^L\right|, \tag{7}$$

$$d^L = \frac{\left|\boldsymbol{b}^L\right|}{\left|E_c\boldsymbol{\xi}^D\right|}\sin\left|\theta^D - \theta^L\right|, \tag{8}$$

where θ^D and θ^L are the angles between ξ^D and ξ^L and x axis, respectively. Then the habit plane indices can be calculated. The habit plane (HP1) can be obtained from the terrace plane by rotation about ξ^D by the angle

$$\psi^1 = \tan^{-1}\frac{h(A)}{d^D}. \tag{9}$$

A second iteration of calculation has to be performed in order to make the results more precise. In order to obtain a new estimation of habit plane (HP2), the calculation is repeated, but the terrace plane is replaced by the previously estimated habit plane, i.e. the coherency strain in HP1 must be balanced by the arrays of defects. The new estimation of rotation angle is

$$\psi^2 = \sin^{-1}\frac{h(A)}{d^{D'}}, \tag{10}$$

where $d^{D'}$ is the spacing of disconnections in HP1.

The results are presented in Table and Fig. 3. The habit planes and defect spacings are listed in Table for 4 symmetry equivalent LID dislocations. The Burgers vectors of these dislocations are differently oriented relative to the terrace plane. Hereby 4 different habit planes can be obtained for each of 4 possible orientation relationships between the austenite and $V3$ variant of martensite. A complete set of 16 habit planes is shown in stereographic projection in Fig. 3. Also, the normals to the experimentally observed interfaces are shown in Fig. 3.

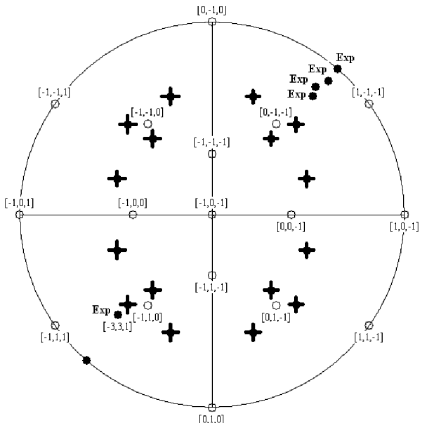

Fig. 3. Stereographic projection of austenite. Theoretical and experimental normal directions to the habit planes between austenite and $V3$ variant of martensite are marked by the crosses and black circles, respectively.

TABLE

Interfaces between austenite and $V3$ variant of martensite for a set of $\boldsymbol{b}^L$ for the terrace plane $(1\bar{1}0)_A//(1\bar{2}1)_M$. Indices are in the austenite coordinate system.

	Austenite–martensite habit plane (HP2)	$d^{D'}$ [Å]	$d^{L'}$ [Å]
$\boldsymbol{b}^L = 1/32\langle 54\bar{3}\rangle$	(1.113, −0.671, 0.0497)	16.0	34.5
$\boldsymbol{b}^L = 1/32\langle 5\bar{4}\bar{3}\rangle$	(1.040, −0.942, −0.170)	15.4	34.0
$\boldsymbol{b}^L = 1/32\langle\bar{5}43\rangle$	(0.736, −1.205, 0.0655)	8.4	11.6
$\boldsymbol{b}^L = 1/32\langle\bar{5}\bar{4}\bar{3}\rangle$	(0.240, −0.420, −1.328)	2.1	8.1

Comparison of the topology model prediction with the experimental data demonstrates a significant disagreement. A reasonable agreement is found only for the case of near {331} habit plane. Other predicted habit planes are inclined from the experimental ones by ≈ 20–30°. Hereby, the results obtained from consideration of topological model are comparable to the results of phenomenological model of martensite [3]. Both approaches predict the existence of {331} habit planes, however, they did not describe all possible habit planes found experimentally. The reason of disagreement can be an influence of local internal strains near the boundaries as it was discussed for instance in [10, 11]. The habit planes can be also affected by the free surfaces since the observations were performed in thin foils.

4. Conclusions

The austenite–single-variant-martensite interfaces in Cu–Al–Ni alloy were considered in the frame of topological model of martensite interfaces. The calculated planes were compared with the habit planes observed in the foils of Cu–Al–Ni alloys deformed *in situ* in a transmission electron microscope. It was shown that the used approach gives reasonable agreement for the $\{331\}_A$ interface planes, but the other observed interface planes were not obtained from this model.

Acknowledgments

Financial support from Grant Agency of ASCR contract number IAA100100920 is gratefully acknowledged.

References

[1] K. Otsuka, K. Shimizu, *Jpn. J. Appl. Phys.* **8**, 1196 (1969).

[2] N. Zarubova, J. Gemperlova, A. Gemperle, Z. Dlabacek, P. Sittner, V. Novak, *Acta Mater.* **58**, 5109 (2010).

[3] K. Bhattacharya, *Microstructure of Martensite*, Oxford University Press, Oxford 2003.

[4] A. Ostapovets, N. Zarubova, V. Paidar, *Int. J. Mater. Res.* **100**, 342 (2009).

[5] R.C. Pond, X. Ma, Y.W. Chai, J.P. Hirth, in: *Dislocations in Solids*, Eds. F.R.N. Nabarro, J.P. Hirth, Elsevier, Amsterdam 2007, p. 225.

[6] R.C. Pond, X. Ma, J.P. Hirth, *J. Mater. Sci.* **43**, 3881 (2008).

[7] X. Ma, R.C. Pond, *J. Mater. Sci.* **46**, 4236 (2011).

[8] S. Ichinose, Y. Funatsu, K. Otsuka, *Acta Metall.* **33**, 1613 (1985).

[9] A. Ostapovets, V. Paidar, *Key Eng. Mater.* **465**, 65 (2011).

[10] G. Maciejewski, S. Stupkiewicz, H. Petryk, *Arch. Mech.* **57**, 277 (2005).

[11] S. Stupkiewicz, G. Maciejewski, H. Petryk, *Acta Mater.* **55**, 6292 (2007).